EVOLUTIONARY AND DETERMINISTIC METHODS FOR DESIGN, OPTIMIZATION AND CONTROL
C. Poloni, D. Quagliarella, J. Périaux, N. Gauger and K. Giannakoglou (Eds.)

SHAPE OPTIMIZATION USING THE AEROSTRUCTURAL COUPLED ADJOINT APPROACH FOR VISCOUS FLOWS

Mohammad Abu-Zurayk*
Institute of Aerodynamics and Flow-Technologies
German Aerospace Center
Lilienthalplatz 7, 38108, Braunschweig, Germany
Email: mohammad.abu-zurayk@dlr.de
web page: http://www.dlr.de/as

Joël Brezillon
Institute of Aerodynamics and Flow-Technologies
German Aerospace Center
Lilienthalplatz 7, 38108, Braunschweig, Germany
Email: joel.brezillon@dlr.de
web page: http://www.dlr.de/as

Abstract. The aero-structural coupled adjoint approach is an efficient approach to compute the gradients of the aerodynamic coefficients obtained from coupled fluid-structure simulations. These gradients can then be advantageously employed for gradient-based optimizations. In this study, the approach is extended for the first time to tackle viscous flows. After introducing the theory, the method is applied to optimize the flight shape of two realistic 3D configurations. In both applications, the coupled adjoint approach permits to decrease the drag at constant lift with limited computational effort.

Key words: MDO, coupled aero-structure adjoint, flight shape, gradient-based optimization, viscous flow.

1 INTRODUCTION

The wing design under aero-elastic effects is increasingly investigated in the aerospace computational sciences. The benefit of taking the aero-elastic deformations into consideration is to consider the influence of the structural flexibility at an early stage in the design process and to perform directly the design on the so called flight shape[1]. The coupling strategy followed in this paper is presented in figure 1. Firstly the aerodynamic loads are computed for the CFD grid by solving the flow equations. Then the loads are transferred to the CSM grid, which in turn is deformed once the structural equations are solved. Since such deformation mainly modifies both the bending and the twist of the wing[2], the structural deformation has to be interpolated back on the CFD grid to update the aerodynamic loads. This process is repeated several times until the system converges, i.e. the deformation does not change between two successive couplings.

Optimizing a wing under the aero-structural effects using gradient-based algorithms is expensive when employing many design variables and the traditional finite differences approach. The cost of the gradients' computation is then linearly dependent on the number of the design variables. Alternatively, the adjoint approach for coupled aero-structural equations allows computing the gradients more efficiently, as already

demonstrated by Mertins et al[3] on a supersonic aircraft for inviscid flows. At DLR, similar approach was adopted and the discrete flow adjoint equations, implemented[4] in the CFD solver TAU[5], were used to develop the aero-structural coupled adjoint approach for inviscid flow. The approach was then successfully applied to optimize the 3D aero-elastic LANN[6] wing[7]. The aim of this paper is to present the formulation of the coupled adjoint approach for viscous flows, and the benefit of the approach in optimizing the flight shape of a wing and a wing-body configuration.

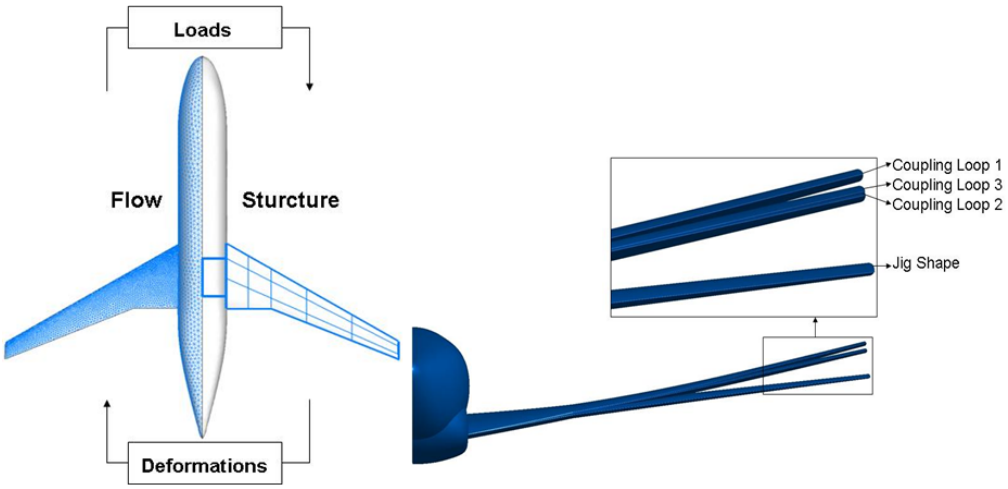

Figure 1: Aero-Structural coupling

2 FORMULATION OF COUPLED ADJOINT

The coupled adjoint approach developed at DLR is based on the TAU code and ANSYS Mechanical[8] which solve the flow equations (Ra=0) and the structure equations (Rs=0) respectively. The flow equations, here described by the Reynolds-Averaged Navier-Stokes equations and completed by the Spalart-Allmaras turbulent model, are solved for the flow state variables (w). On the other hand, the structure equations, as described by the linear equation (1), are solved for the structural deformation (u), where (f) and (K) represent the structural loads and the stiffness matrix, respectively.

$$Rs = f - Ku = 0 \tag{1}$$

We now consider a generic cost function (I), defined as a function of the coupled state variables vector W=[w u] and the total set of design variables vector D=[A T], where (A) and (T) are the design variables for the aerodynamic shape and the structural thickness, respectively. Similarly we define the coupled residual vector R=[Ra Rs]. The gradients of the cost function (I) with respect to the vector of design variables (D) can then be defined in the vector format as:

$$\frac{dI}{dD} = \frac{\partial I}{\partial D} + \begin{bmatrix} \frac{\partial I}{\partial w} & \frac{\partial I}{\partial u} \end{bmatrix} \begin{bmatrix} \frac{dw}{dD} \\ \frac{du}{dD} \end{bmatrix} \tag{2}$$

and the gradients of the residual vector R=[Ra Rs] with respect to the set of design variables (D) has the same form as in equation (2).

To formulate the coupled adjoint equation, a Lagrange (L) is defined in equation (3)

$$L = I + \Psi R \tag{3}$$

where (Ψ) is the Lagrange multipliers vector Ψ=[ψ φ] that contains both the aerodynamic (ψ) and the structure (φ) Lagrange multipliers. Since the residual vector R is equal to zero per definition, the gradients of the Lagrange are equal to the gradients of the cost function and can be written in the vector form as:

$$\frac{dL}{dD}=\frac{dI}{dD}=\left(\begin{bmatrix}\frac{\partial I}{\partial A}\\ \frac{\partial I}{\partial T}\end{bmatrix}+\begin{bmatrix}\frac{\partial Ra}{\partial A} & \frac{\partial Rs}{\partial A}\\ \frac{\partial Ra}{\partial T} & \frac{\partial Rs}{\partial T}\end{bmatrix}\begin{bmatrix}\psi\\ \phi\end{bmatrix}\right)\begin{pmatrix}\frac{dA}{dD} & \frac{dT}{dD}\end{pmatrix}+\left(\begin{bmatrix}\frac{\partial I}{\partial w}\\ \frac{\partial I}{\partial u}\end{bmatrix}+\begin{bmatrix}\frac{\partial Ra}{\partial w} & \frac{\partial Rs}{\partial w}\\ \frac{\partial Ra}{\partial u} & \frac{\partial Rs}{\partial u}\end{bmatrix}\begin{bmatrix}\psi\\ \phi\end{bmatrix}\right)\begin{pmatrix}\frac{dw}{dD} & \frac{du}{dD}\end{pmatrix} \tag{4}$$

The second term of equation (4) includes the computationally expensive terms (dw/dD) and (du/dD) which require a flow and a structure computation for each design variable when approximated with the finite-differences approach. For this reason, the Lagrange multipliers vector Ψ is chosen such that

$$\begin{bmatrix}\frac{\partial I}{\partial w}\\ \frac{\partial I}{\partial u}\end{bmatrix}+\begin{bmatrix}\frac{\partial Ra}{\partial w} & \frac{\partial Rs}{\partial w}\\ \frac{\partial Ra}{\partial u} & \frac{\partial Rs}{\partial u}\end{bmatrix}\begin{bmatrix}\psi\\ \phi\end{bmatrix}=0 \tag{5}$$

Equation (5) is called the coupled adjoint equation and the Lagrange multipliers (ψ) and (ϕ) are called the adjoint variables. It is worth mentioning that this equation is solved independently of the number of design parameters. Following this approach, the gradient of the function (I) is reduced to:

$$\frac{dI}{dD}=\left(\begin{bmatrix}\frac{\partial I}{\partial A}\\ \frac{\partial I}{\partial T}\end{bmatrix}+\begin{bmatrix}\frac{\partial Ra}{\partial A} & \frac{\partial Rs}{\partial A}\\ \frac{\partial Ra}{\partial T} & \frac{\partial Rs}{\partial T}\end{bmatrix}\begin{bmatrix}\psi\\ \phi\end{bmatrix}\right)\begin{pmatrix}\frac{dA}{dD}\\ \frac{dT}{dD}\end{pmatrix} \tag{6}$$

This means that the coupled aero-structural sensitivities are obtained after solving one aero-structure coupled residual, one coupled adjoint equation, in addition to the computation of (6).

A more detailed explanation about the derivation of the terms, and the strategy followed in solving those equations for inviscid flow can be found in reference[7].

The paper now focuses on the extension of the coupled adjoint approach in order to tackle viscous flows. To carry out this extension, it was required to adapt the adjoint boundary condition (∂I/∂w) which represents the sensitivity of the cost function with respect to the change in the flow state variables. The other terms that are required to extend to viscous flows were the terms (∂I/∂u) and (∂Ra/∂u) which correspondingly represent the sensitivities of the cost function and the aerodynamic residuals with respect to the change in the structural deformation. These terms are expressed, using the chain rule, as:

$$\frac{\partial I}{\partial u}=\frac{\partial I}{\partial Xa}\frac{\partial Xa}{\partial u}$$
$$\frac{\partial Ra}{\partial u}=\frac{\partial Ra}{\partial Xa}\frac{\partial Xa}{\partial u} \tag{7}$$

where (Xa) represents the volume CFD mesh. The term (∂Xa/∂u) represents the sensitivity of the CFD mesh with respect to the change in the structural deformation and was previously obtained after differentiating the interpolation tool[7]. The remaining terms are the viscous metric terms, namely (∂I/∂Xa) and (∂Ra/∂Xa). They were originally derived during the development of the adjoint equation for the mesh deformation[9] and are here reused for solving the coupled adjoint equations. Once all terms are available, the coupled adjoint equations are solved using the lagged iterative method[3].

The coupling between the two solvers; TAU and ANSYS Mechanical, employs the interpolation tool[10] available in TAU. This tool uses a linear interpolation algorithm to transfer the aerodynamic loads from the CFD grid to the CSM grid, and a radial basis function (RBF), based on the volume spline, to transfer the structural deformations in the opposite direction.

In the following applications, structural design parameters like the thickness of the structural elements are not taken into account, which means that structural elements are frozen during the optimization but the effect of the static structural deformation is taken into account.

3 APPLICATION ON VISCOUS AERO-ELASTIC WING

For this first application, the LANN wing is selected and the impact of the viscosity in flow simulation is first highlighted. For that purpose Euler and RANS computations are performed on the LANN wing at an angle of incidence of 0° and a Mach number of 0.82 and $7.3*10^6$ Reynolds number for the viscous computation. The computations are here performed without structure coupling in order to allow a fair comparison to the experimental results. Figure 2 presents the resulting pressure distribution and clearly emphasizes the importance of considering viscous flows to accurately predict the shock position. In light of this result, a wing design has to take into account the fluid's viscosity in order to properly modify the shape in the appropriate area.

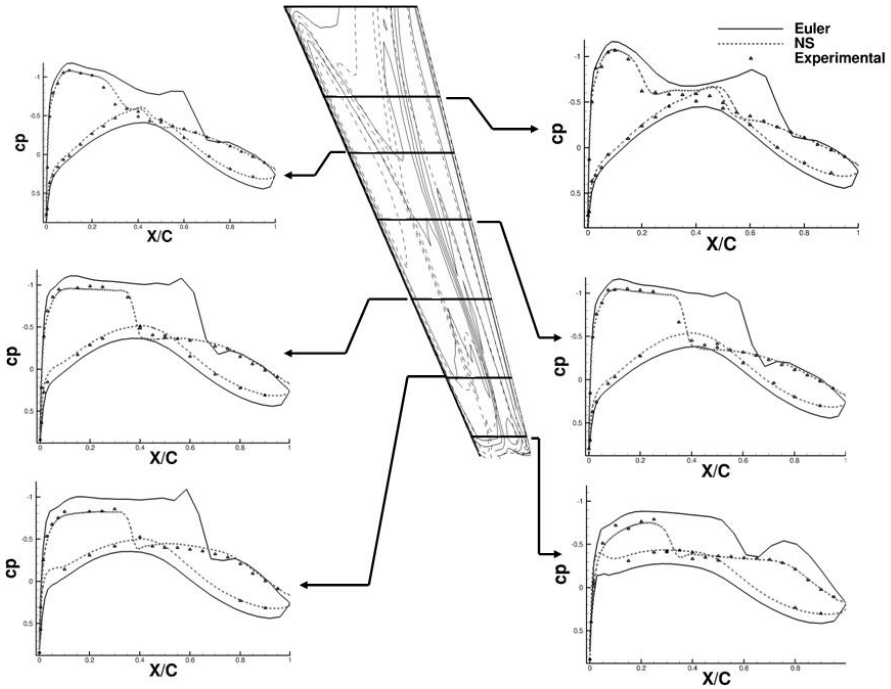

Figure 2: Cp of LANN wing, for inviscid and viscous computations compared to experimental results

We now consider the aero-elastic wing and figure 3 presents the CFD and the CSM grids that are used during the coupling. The CFD grid is made of hexahedra elements and contains around 1.2 million nodes. The CSM grid is modeled with around 9000 nodes using triangular and rectangular beam elements, where each node has 6 degrees of freedom; 3 translational (x, y, z) and 3 rotational (θ_x, θ_y, θ_z). The wing shape is parameterized using the freeform deformation[11] (FFD) box with 60 shape design variables, equally divided over the upper and the lower surfaces of the wing. The flow computations are performed at a Mach number of 0.82 and a Reynolds number of $7.3*10^6$ while keeping the lift constant at $C_L = 0.6$ by adjusting the angle of attack. To model the turbulence, the Spalart-Allmaras one-equation model is used.

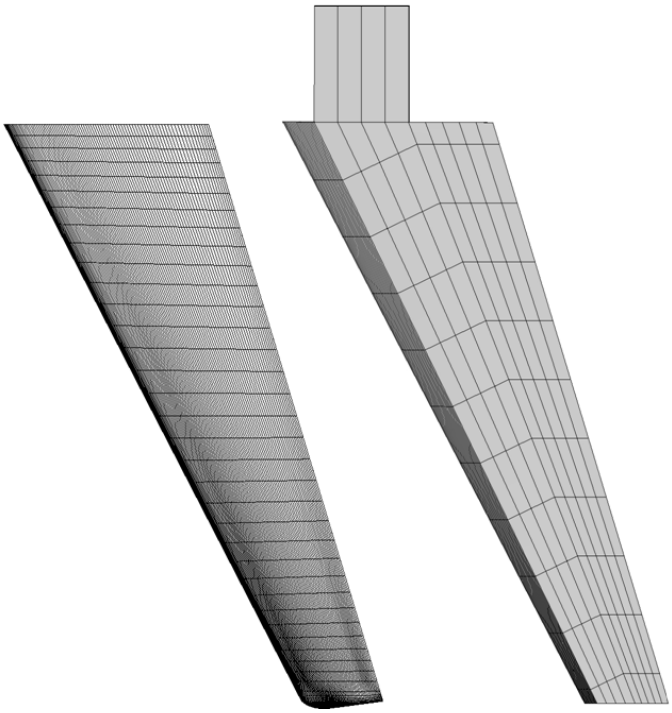

Figure 3: CFD (left) and CSM (right) grids of the LANN wing

3.1 Gradients Evaluation

Before starting the optimization, the accuracy of the cost function's gradients with respect to the design parameters is checked. As a reference for this evaluation, the central finite differences (FD) are considered. To ensure the reliability of using the finite differences, several FD steps were tested and only the right range of steps is presented and used for the evaluation.

The design parameters used in this verification are 20 FFD parameters. The cost function used is drag at constant lift, and it is the same cost function that's intended for the optimization. To compute the gradients of the drag at constant lift, the variations of drag and lift are first expressed by differencing explicitly the components due to the shape (D) and the angle of attack (α):

$$\delta C_D \approx \frac{\partial C_D}{\partial D}\delta D + \frac{\partial C_D}{\partial \alpha}\delta\alpha \tag{8}$$

$$\delta C_L \approx \frac{\partial C_L}{\partial D}\delta D + \frac{\partial C_L}{\partial \alpha}\delta\alpha \tag{9}$$

In order to maintain the lift constant during the optimization, the angle of attack has to be adapted to exactly compensate the modification introduced by the shape. As a consequence equation (9) should be equal to zero and the variation of (α) is then defined as:

$$\delta\alpha = (\frac{\partial C_L}{\partial D}\delta D) / (\frac{\partial C_L}{\partial \alpha}) \tag{10}$$

By introducing this term into equation (8), the gradients of the drag at constant lift becomes:

$$\frac{d(C_D)@\text{ constant Lift}}{dD} = \frac{dC_D}{dD} - (\frac{dC_D}{d\alpha} / \frac{dC_L}{d\alpha})\frac{dC_L}{dD} \tag{11}$$

To compute the terms (dC_D/dD) and (dC_L/dD), two coupled adjoint computations are required; one for drag and one for lift. The terms ($dCD/d\alpha$) and ($dC_L/d\alpha$) have been differentiated per hand and are provided by the TAU solver at the end of the adjoint computations.

On the other hand, for the central finite differences, the gradients are based on flow computations with target lift for each design variable.

The resulting gradients of the LANN's flight shape are presented in figure 4. The figure shows a very good matching between the finite differences and the coupled adjoint gradients. To emphasize the benefit of the method, it is worth mentioning here that the time needed for computing the gradients with the adjoint approach was around 10% of that needed by the finite differences approach.

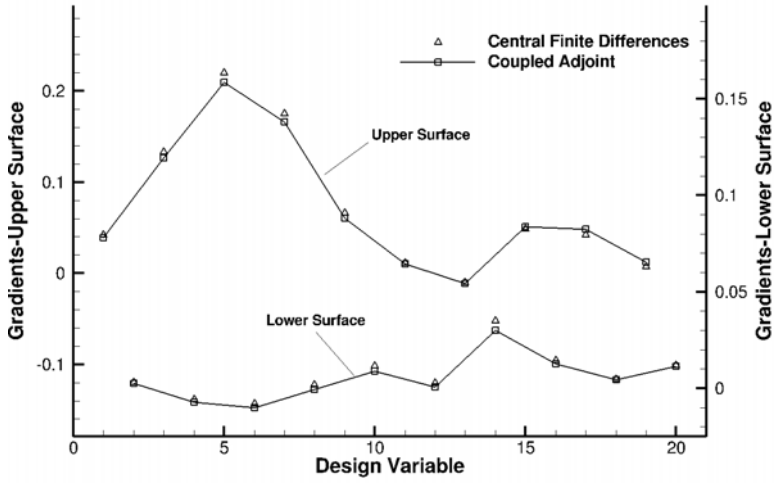

Figure 4 : Gradients evaluation for LANN wing; comparison between finite differences and coupled adjoint

3.2 Optimization

The optimization aims to reduce the drag of the LANN's flight shape at a constant lift and thickness. To ensure constant thickness, every pair of upper and lower design variables were linked such that they move with the same displacement. The optimization process is controlled by a Python-based environment[12] and a conjugate gradient algorithm is employed as optimizer.

Figure 5 presents the convergence of the optimization, where the drag is reduced by around 64% of its initial value, while the lift and the thickness are kept constant. The optimization is fully converged after 30 aero-structural coupled simulations and 8 gradient computations and took in total 25 hours wall clock on 32 processors.

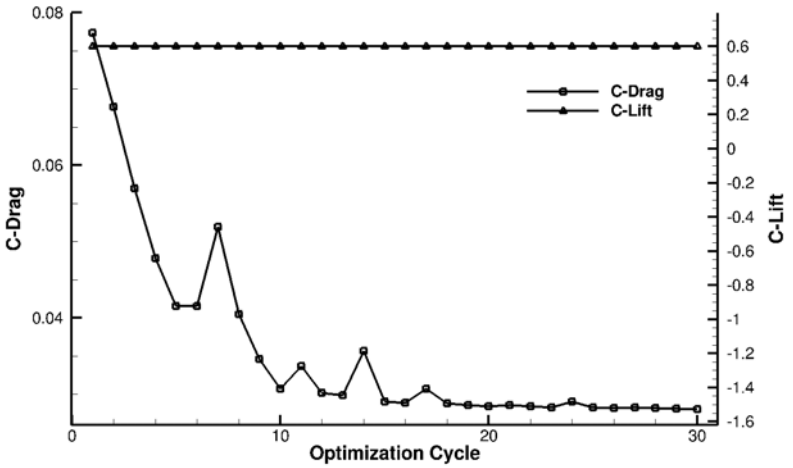

Figure 5: Convergence history of LANN wing optimization

Figure 6 presents the top and the front views of the initial and optimized LANN wing, showing the pressure contour for the flight shape configurations. The top view illustrates how the shock was drastically reduced and the front view shows that the optimized shape experiences a higher bending than the initial one.

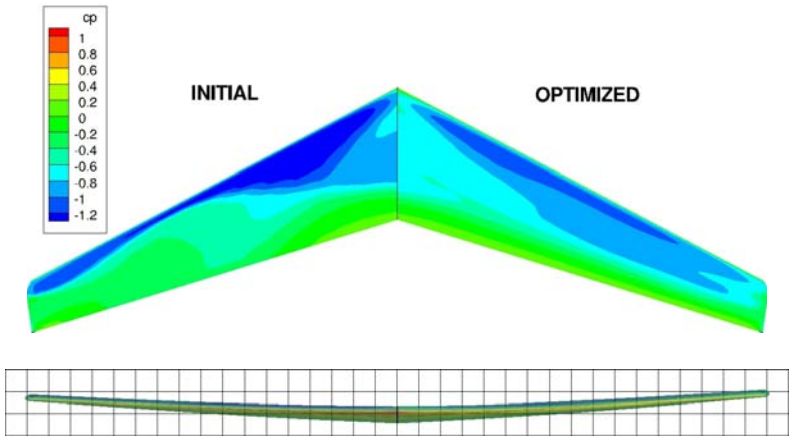

Figure 6: Cp of initial and optimized configurations; Top and front view of the LANN wing

Figure 7 presents a closer look at the pressure distribution at different wing sections for the initial and the optimized flight shapes. The shock is clearly reduced as the figure shows.

4 APPLICATION ON VISCOUS WING-BODY CONFIGURATION

The wing-body configuration presented in figure 8 is now considered. The configuration is derived from the Do728 geometry and was constructed in the frame of the DLR internal project MDOrmec which deals with multidisciplinary optimization of a rear mounted engine configuration[13]. The configuration was originally designed with an engine under the wing, and therefore presents a large potential for drag reduction.

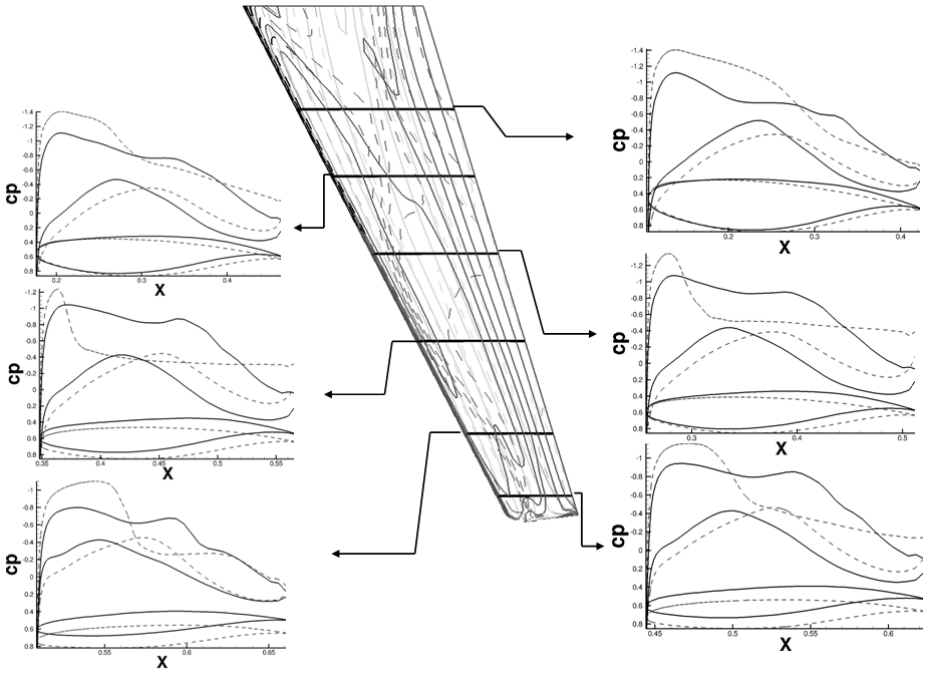

Figure 7: Cp of initial (dashed lines) and optimized (solid lines) wings

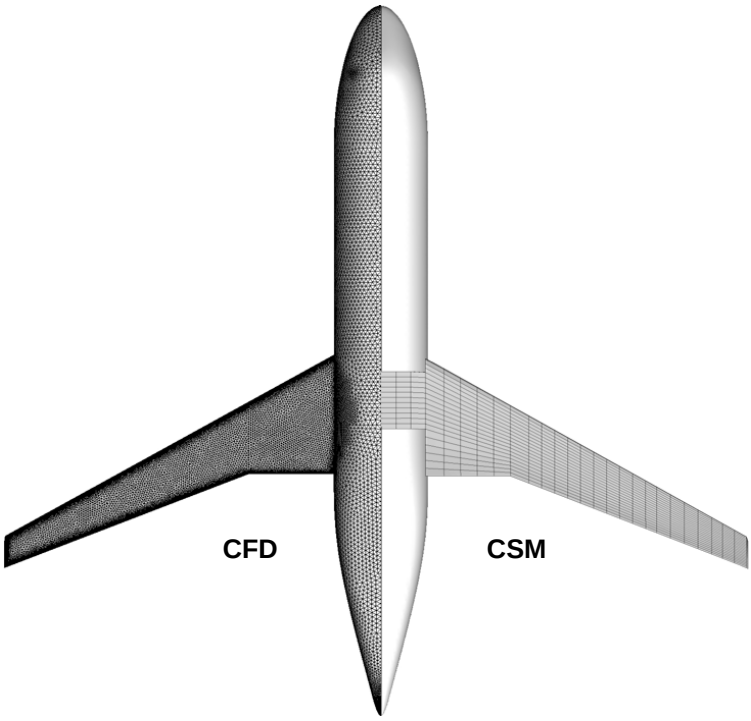

Figure 8: CFD and CSM grids of the wing-body configuration

For this optimization, the CSM and the unstructured CFD grid contain around 4000 and 1.7 million nodes, respectively. The CSM grid is modeled using rectangular beam elements, where the nodes of each element have 6 degrees of freedom.

For this application, the flow variables are computed at a Mach number of 0.82, a Reynolds number of $21*10^6$ and a constant lift of $C_L = 0.554$. The one equation turbulence model, Spalart-Allmaras is employed. The wing is parametrised with 80 FFD design parameters; equally divided on the upper and the lower surfaces of the wing.

As in the previous application, the gradients were initially evaluated, and then the

optimization took place. Figure 9 shows the gradients of the drag at constant lift with respect to 7 selected design parameters. The coupled adjoint gradients match nicely with the central finite differences gradients as the figure shows.

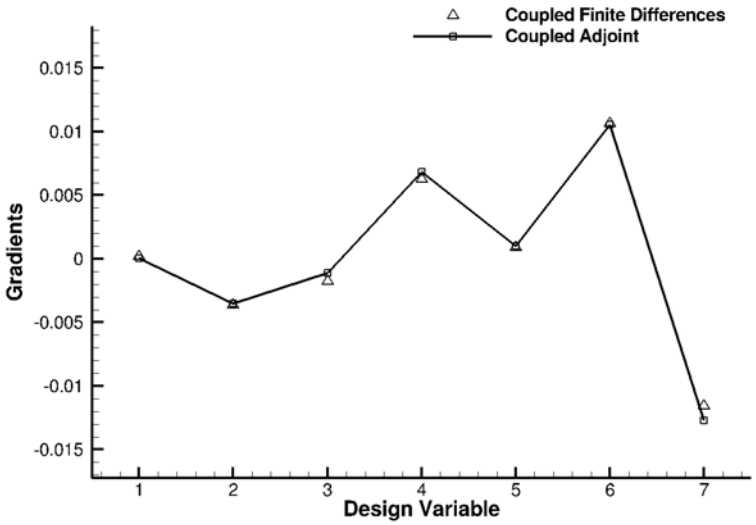

Figure 9: Evaluation of the gradients for the wing-body configuration

Figure 10 presents the optimization's convergence for the viscous wing-body configuration, where the drag is reduced by around 19% of its initial value while the lift is kept constant. The optimization took 75 hours on 96 processors. It needed 35 coupled fluid-structure and 11 coupled adjoint computations to converge.

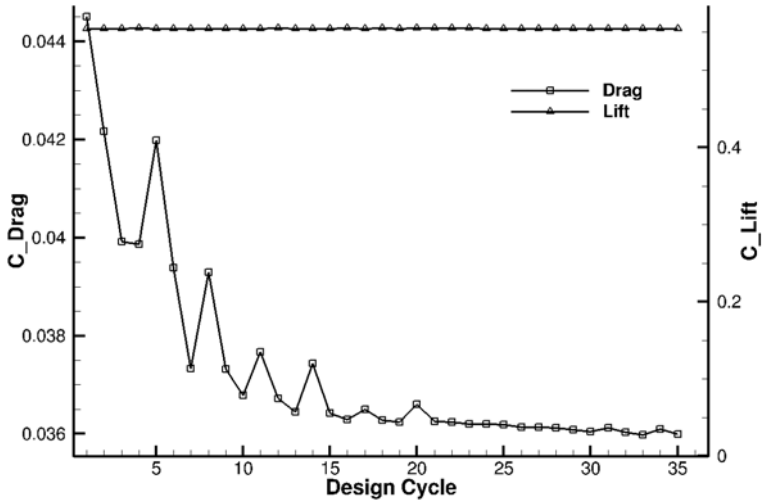

Figure 10: Convergence history for the optimization of wing-body configuration

Figure 11 presents the top and the front views of the pressure contour for the flight shape configurations at both the initial and the optimized designs. The top view illustrates how the shock was reduced, and the front view shows a higher bending in the optimized shape when compared to the initial shape.

A closer look at the pressure distributions for different sections confirms the shock reduction as presented in figure 12.

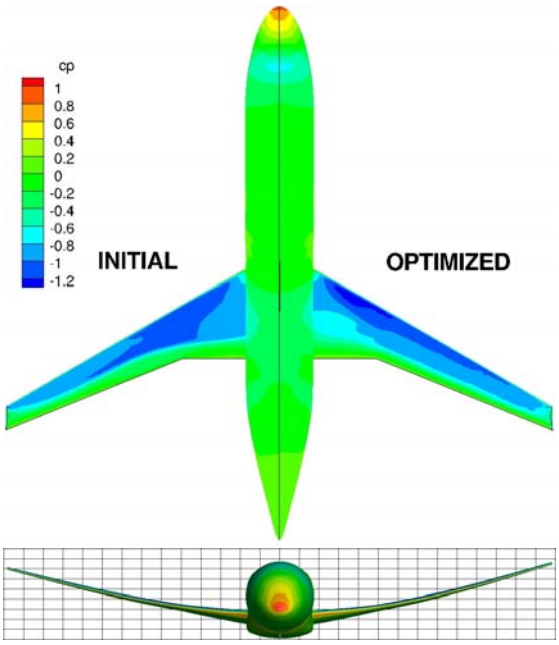

Figure 11: Cp contour of the initial and optimized wing-body configurations

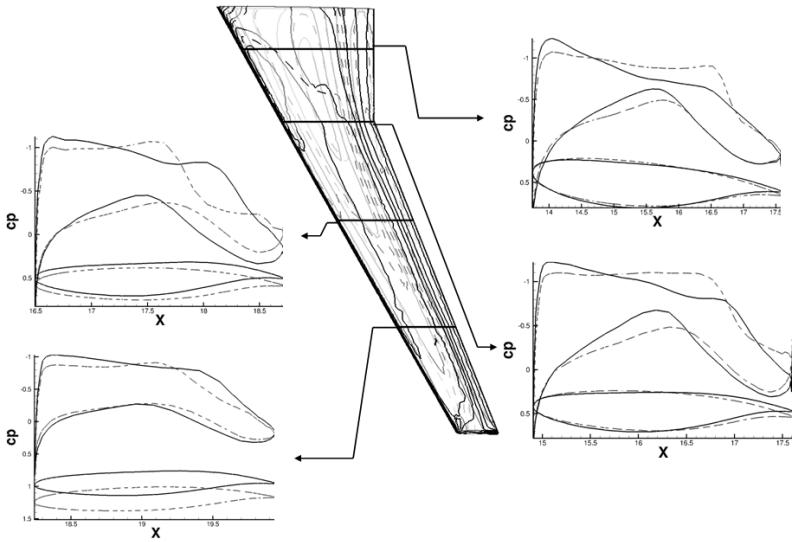

Figure 12: Cp of the initial (dashed lines) and optimized (solid lines) configurations

5 CONCLUSIONS

The coupled adjoint approach was developed to efficiently perform sensitivity analysis and to speed up the design of aero-structural coupled problems. The approach employs DLR's TAU code to solve the flow equations and ANSYS Mechanical to solve the structure equations. In the paper, the approach was further developed to tackle viscous flows. The resulting gradients match well with the central finite differences' gradients, and are accurate enough to successfully optimize the flight shape of a wing and a wing-body configuration in a limited turn around time. Such approach is therefore a promising tool for the wing shape design.

6 FUTURE WORK

The work on the coupled adjoint will be extended in the next steps in order to include structural design variables, and correspondingly structural cost functions in the developed approach.

7 ACKNOWLEDGEMENT

The authors would like to thank Markus Widhalm who has made a valuable contribution to this paper by deriving the viscous metric terms mentioned in section 2. We also want to thank Arno Ronzheimer and Josef Natterer for providing the CFD and CSM grids of the wing-body configuration.

8 REFERENCES

[1] P. Flick, M. Love, P. Zink, *The Impact of Active Aeroelastic Wing Technology on Conceptual Aircraft Design,* RTO AVT Specialists' Meeting, Canada (1999).

[2] N. Gross, *ETW Analytical approach to assess the wing twist of pressure plotted wind tunnel models*, AIAA 2002-0310 (2002).

[3] J. Martins, J. Alonso, J. Reuther, *A Coupled-Adjoint Sensitivity Analysis Method for High-Fidelity Structural Design*, Optimization and Engineering, 6, 33-62, (2005).

[4] R. Dwight, *Efficiency Improvement of RANS-Based Analysis and Optimization Using Implicit and Adjoint Methods on Unstructured Grids,* DLR Forschungsbericht, ISSN 1434-8454, Report 2006-11, (2006).

[5] T. Gerhold. *Overview of the Hybrid RANS code TAU*, In: Kroll, N., Fassbender, J.K. Notes on Numerical Fluid Mechanics and Multi-disciplinary Design, vol. 89, pp. 81-92. Springer, Heidelberg (2005).

[6] R. J. Zwaan*, Data Set 9, LANN Wing. Pitching Oscillation, AGARD.* Repr. R-702, Addendum No.1 (1985).

[7] M. Abu-Zurayk, J. Brezillon, *Development and evaluation of the adjoint approach for aeroelstic wing optimization,* 17 DGLR-Fach-Symposium der STAB, (2010).

[8] *www.ansys.com*

[9] M. Widhalm, J. Brezillon, C. Ilic, T. Leicht, *Investigation on Adjoint Based Gradient Computations for Realistic 3d Aero-Optimization,* 13th AIAA/ISSMO Multidisciplinary Analysis Optimization Conference, (2010).

[10] N. Kroll, R. Heinrich, W. Krueger, B. Nagel, *Fluid-Structure Coupling for Aerodynamic Analysis and Design: A DLR Perspective*, AIAA 2008-561 (2008).

[11] A. Ronzheimer, *Shape parameterization Using Freeform Deformation*. In: MEGAFLOW- Numerical Flow Simulation for Aircraft Design, ISBN 3-540-24383-6 (2005).

[12] J. Brezillon, M. Abu-Zurayk, *Aerodynamic Inverse Design Framework using Discrete Adjoint Method,* 17 DGLR-Fach-Symposium der STAB. (2010).

[13] A. Ronzheimer, F.J. Natterer, J. Brezillon, *Aircraft Wing Optimization Using High Fidelity Closely Coupled CFD and CSM Methods*, 13th AIAA/ISSMO Multidisciplinary Analysis Optimization Conference, Fort Worth, Texas. (2010).